ATTITUDE ESTIMATION PROCESS OF THE SENSING REMOTE SATELLITE CBERS-2 WITH UNSCENTED KALMAN FILTER AND QUATERNION INCREMENTAL, USING REAL DATA

R. V. Garcia[(1)], H. K. Kuga[(2)], M. C. Zanardi[(3)], and N. F. O. Matos[(4)]

[(1)] *Universidade de São Paulo, Lorena School of Engineering, Department of Environmental Sciences, São Paulo, Lorena, CEP: 12602-810, Brazil, phone: 55(12)3159-5000, robertagarcia@usp.br*

[(2)] *Brazilian Institute for Space Research (INPE), Space Mechanics and Control Division, São Paulo, Sao José dos Campos, CEP: 12227-010, Brazil, phone: 55(12)3208-6000, hkk@dem.inpe.br*

[(3)] *Universidade Federal do ABC, São Paulo, Santo André, CEP: 09.210-580, Brazil, email mceciliazanardi@gmail.com*

[(4)] *Sao Paulo State University (UNESP), Department of Mathematics, Group of Orbital Dynamics and Planetology, São Paulo, Guaratinguetá, CEP: 12516-410, Brazil, phone: 55(12)3123-2194, nicholas.f.matos@hotmail.com*

Abstract: *This work is related to the dynamics of rotational motion of artificial satellites, that is, its orientation (attitude) with respect to an inertial reference system. The attitude determination process, in general, involves the knowledge of nonlinear estimation techniques and is essential to the safety and control of the satellite and payload. The aim of this work is to study the influence of real data of the CBERS-2 (China Brazil Earth Resources Satellite) satellite in the attitude estimation process when the estimator is the Unscented Kalman Filter (UKF) and the attitude is represented by quaternion incremental. The attitude sensors available are DSS (Digital Sun Sensor), IRES (Infrared Earth Sensor), and the gyros. For nonlinear systems, the UKF uses a carefully selected set of sample points to map the probability distribution more accurately than the linearization of the standard Extended Kalman Filter (EKF). Herein the proposal is to estimate the attitude and the drift of the gyros obtained by the UKF and EKF with quaternion incremental and compare them. The results show that, although the EKF and UKF have roughly the same accuracy, the UKF leads to a convergence of the state vector faster than the EKF. This fact was expected, since the UKF prevents the linearizations needed for EKF, when the system has some nonlinearity in their equations.*

Keywords: *Unscented Kalman Filter, real data, attitude estimation, quaternion, Extended Kalman Filter.*

1. Introduction

Nonlinearities in spacecraft attitude determination problem have been studied intensively during the past decades. To resolve this kind of problem the extended Kalman filter (EKF) algorithm has proven to be a successful solution for engineering application. Unfortunately, the EKF has two important drawbacks: the linear approximators to the nonlinear function can be complex causing implementation difficulties, and these linearizations can lead to filter instability if the timestep intervals are not sufficiently small. In recent years, advances in space missions, such as the greater agility, demand and the application of lower cost sensors, deserve a revisit of the nonlinearity issue. In the existing methods, the Sigma-Point Kalman filters (SPKF) have proven

to be among the most efficient ones. In this work one of the SPKF family algorithms, called Unscented Kalman Filter, is used.

A widely used parameterization for attitude estimation is the quaternion representation. Some advantages of using quaternions include: linear kinematic equations with respect to angular velocities, absence of singularities for any axis rotation, and the algebraic attitude matrix in the quaternion components. However, since the quaternion parameterization involves the use of four components to represent the attitude motion, the quaternion components are dependents, which leads to a constraint that the quaternion must have a unit norm. This constraint produces a singularity in the Kalman filter covariance matrix. To resolve this problem, here is used an incremental quaternion error. This approach is most commonly used to maintain normalization for the estimated quaternion [5].

2. Unscented Kalman Filter

The basic premise behind the Unscented Kalman Filter (UKF) is that it is easier to approximate a Gaussian distribution than it is to approximate an arbitrary nonlinear function. Instead of linearizing using Jacobian matrices, the UKF uses a deterministic sampling approach to capture the mean and covariance estimates with a minimal set of sample points [4]. Here we present an algorithmic description of the UKF omitting some theoretical considerations. More details can be found in [2] [4].

Consider the nonlinear system model given by:

$$\begin{aligned} \dot{\boldsymbol{x}}_k &= f(\boldsymbol{x}_k, k) + G_k \boldsymbol{w}_k \\ \boldsymbol{y}_k &= h(\boldsymbol{x}_k, k) + \boldsymbol{v}_k \end{aligned} \tag{1}$$

where $\boldsymbol{x}_k$ is the n x 1 state vector and $\boldsymbol{y}_k$ is the m x 1 measurement vector. The function f is a possible nonlinear function of the state $\boldsymbol{x}_k \in \Re^n$ and the observation $\boldsymbol{y}_k \in \Re^m$ is often a nonlinear mapping of the current state. Both the dynamic model and the measurement model are inaccurate, due to modeling and/or sensor errors. This is described by the stochastic processes in which we assume that the process noise $\boldsymbol{w}_k$ and measurement-error noise $\boldsymbol{v}_k$ are zero-mean Gaussian noise process with covariance given by Q_k and R_k, respectively.

Given the state vector and the covariance matrix at step k-1, we compute a collection of sigma points, stored in the columns of the n x $(2n+1)$ sigma point matrix $\boldsymbol{\chi}_{k-1}$ where n is the dimension of the state vector. The columns of $\boldsymbol{\chi}_{k-1}$ are computed by:

$$\begin{aligned} (\boldsymbol{\chi}_{k-1})_0 &= \hat{\boldsymbol{x}}_{k-1} \\ (\boldsymbol{\chi}_{k-1})_i &= \hat{\boldsymbol{x}}_{k-1} + \left(\sqrt{(n+\lambda)\mathrm{P}_{k-1}}\right)_i \qquad i = 1,\ldots,n \\ (\boldsymbol{\chi}_{k-1})_i &= \hat{\boldsymbol{x}}_{k-1} - \left(\sqrt{(n+\lambda)\mathrm{P}_{k-1}}\right)_{i-n} \qquad i = n+1,\ldots 2n \end{aligned} \tag{2}$$

in which $\lambda \in \Re$, $\left(\sqrt{(n+\lambda)\mathrm{P}_{\mathrm{k-1}}}\right)_{\mathrm{i}}$ is the *ith* column of the matrix square root of $(n+\lambda)$ $\mathrm{P}_{\mathrm{k-1}}$ and the scalar λ is a convenient parameter for exploiting knowledge about the higher moments of the given distribution. Note that we assume matrix $\left(\sqrt{(n+\lambda)\mathrm{P}_{\mathrm{k-1}}}\right)_{\mathrm{i}}$ as symmetric and positive definite which allows us to find the square root using the Cholesky decomposition.

Once $\boldsymbol{\chi}_{\mathrm{k-1}}$ computed, the sigma points are propagated through the nonlinear system

$$(\boldsymbol{\chi}_{\mathrm{k}})_i = f\left((\boldsymbol{\chi}_{\mathrm{k-1}})_i\right), \qquad i = 0,...2n, \tag{3}$$

The posterior mean, $\hat{\boldsymbol{x}}_{\mathrm{k}}^{-}$, and covariance, $\mathrm{P}_{\mathrm{k}}^{-}$, are determined from the statistics of the propagated sigma points as follows

$$\hat{\boldsymbol{x}}_{\mathrm{k}}^{-} = \sum_{i=0}^{2n} W_i (\boldsymbol{\chi}_{\mathrm{k}})_i \tag{4}$$

$$\mathrm{P}_{\mathrm{k}}^{-} = \sum_{i=0}^{2\mathrm{n}} W_i \left[(\boldsymbol{\chi}_{\mathrm{k}})_i - \hat{\mathbf{x}}_{\mathrm{k}}^{-}\right]\left[(\boldsymbol{\chi}_{\mathrm{k}})_i - \hat{\mathbf{x}}_{\mathrm{k}}^{-}\right]^{\mathrm{T}} + Q_{\mathrm{k}} \tag{5}$$

where the weights are defined by: $W_0 = \dfrac{\lambda}{(n+\lambda)}$, $W_i = \dfrac{1}{2(n+\lambda)}$ $, i = 1,....,2n$.

To compute the correction step, first we must transform the columns of $\boldsymbol{\chi}_{\mathrm{k}}$ through the measurement function to $\boldsymbol{\Upsilon}_{\mathrm{k}}$. In this way

$$\begin{aligned} (\boldsymbol{\Upsilon}_{\mathrm{k}})_i &= h\left((\boldsymbol{\chi}_{\mathrm{k}})_i\right), \qquad i = 0,...2n \\ \hat{\mathbf{y}}_{\mathrm{k}}^{-} &= \sum_{i=0}^{2\mathrm{n}} W_i (\boldsymbol{\Upsilon}_{\mathrm{k}})_i \end{aligned} \tag{6}$$

With the mean measurement vector, $\hat{\mathbf{y}}_{\mathrm{k}}^{-}$, we compute the *a posteriori* state estimate using

$$\hat{\boldsymbol{x}}_k = \hat{\boldsymbol{x}}_k^{-} + K_k \left(\boldsymbol{y}_k - \hat{\boldsymbol{y}}_k^{-}\right) \tag{7}$$

where K_{k} is the Kalman gain. In the UKF formulation, the Kalman gain is defined by

$$K_k = P_{xy} P_{yy}^{-1} \tag{8}$$

with

$$P_{xy} = \sum_{i=0}^{2n} W_i \left[(\boldsymbol{\chi}_k)_i - \hat{\boldsymbol{x}}_k^- \right] \left[(\boldsymbol{Y}_k)_i - \hat{\boldsymbol{y}}_k^- \right]^T \tag{9}$$

$$P_{yy} = \sum_{i=0}^{2n} W_i \left[(\boldsymbol{\Upsilon}_k)_i - \hat{\boldsymbol{y}}_k^- \right] \left[(\boldsymbol{\Upsilon}_k)_i - \hat{\boldsymbol{y}}_k^- \right]^T + R \tag{10}$$

Finally, the last calculation in the correction step is to compute the a posterior estimate of the error covariance given by

$$\mathrm{P_k} = \mathrm{P_k^-} - K_\mathrm{k}\, \mathrm{P_{yy}}\, K_\mathrm{k}^\mathrm{T} \tag{11}$$

3. Attitude Representation by Quaternions

The quaternions are useful in inertial navigation systems on board the satellite, show no singularities in the kinematic equations, give a rule of algebraic products suitable for successive rotations, and the rotation matrix in terms of the quaternion does not depend on trigonometric functions. However, the quaternions have one redundant component (they are 4) with reference to Euler angles (they are 3) and does not have an immediate physical interpretation.

The quaternion set is defined by

$$\mathrm{q} \equiv \left[\mathbf{q}^\mathrm{T} \;\; \mathrm{q}_4 \right]^\mathrm{T} \tag{12}$$

with $\mathbf{q} \equiv \left[\mathrm{q}_1 \;\; \mathrm{q}_2 \;\; \mathrm{q}_3 \right]^\mathrm{T} = \hat{\mathbf{e}} \sin\left(\vartheta / 2 \right)$ and $\mathrm{q}_4 = \cos\left(\vartheta / 2 \right)$,

where $\hat{\mathbf{e}}$ is the axis of rotation and ϑ is the angle of rotation. Since a four-dimensional vector is used to describe three dimensions, the quaternion components cannot be independent from each other. The quaternion satisfies a single constraint given by $\mathrm{q}^\mathrm{T}\,\mathrm{q} = 1$. The attitude matrix is related to the quaternion by [8]:

$$\mathrm{T(q)} = \begin{bmatrix} \mathrm{q}_1^2 - \mathrm{q}_2^2 - \mathrm{q}_3^2 + \mathrm{q}_4^2 & 2(\mathrm{q}_1 \mathrm{q}_2 + \mathrm{q}_3 \mathrm{q}_4) & 2(\mathrm{q}_1 \mathrm{q}_3 - \mathrm{q}_2 \mathrm{q}_4) \\ 2(\mathrm{q}_1 \mathrm{q}_2 - \mathrm{q}_3 \mathrm{q}_4) & -\mathrm{q}_1^2 + \mathrm{q}_2^2 - \mathrm{q}_3^2 + \mathrm{q}_4^2 & 2(\mathrm{q}_2 \mathrm{q}_3 + \mathrm{q}_1 \mathrm{q}_4) \\ 2(\mathrm{q}_1 \mathrm{q}_3 + \mathrm{q}_2 \mathrm{q}_4) & 2(\mathrm{q}_2 \mathrm{q}_3 - \mathrm{q}_1 \mathrm{q}_4) & -\mathrm{q}_1^2 - \mathrm{q}_2^2 + \mathrm{q}_3^2 + \mathrm{q}_4^2 \end{bmatrix} \tag{13}$$

The quaternion kinematics equation is given by:

$$\dot{\mathrm{q}}(\mathrm{t}) = \frac{1}{2} \Omega(\hat{\boldsymbol{\omega}})\, \mathrm{q}(\mathrm{t}) \tag{14}$$

with: $\Omega(\boldsymbol{\omega}) = \begin{pmatrix} 0 & \omega_z & -\omega_y & \omega_x \\ -\omega_z & 0 & \omega_x & \omega_y \\ \omega_y & -\omega_x & 0 & \omega_z \\ -\omega_x & -\omega_y & -\omega_z & 0 \end{pmatrix}$

A major advantage of using the quaternion is that the kinematics equation is linear in the quaternion and is also free of singularities. In this paper, it is assumed that the gyro data are assembled in a fixed rate and that the angular spin velocity vector in a satellite system,$\boldsymbol{\omega}$, is constant over the interval of sampling. Then a solution of Eq. (14) is [3], [5]:

$$q(t_k) = \Phi_q(\Delta t, \boldsymbol{\omega})\, q(t_{k-1}) \tag{15}$$

where Δt is the sampling interval; $q(t_{k-1})$ is the quaternion at time t_{k-1}; $q(t_k)$ is the propagated quaternion to time t_k; e Φ_q is the transition matrix that computes the system from time t_{k-1} to t_k. When the direction of $\boldsymbol{\omega}(t)$ is constant throughout the time interval or the displacements of the axes is small, then Φ_q can be approximated by [5]

$$\Phi_q(\Delta t, \boldsymbol{\omega}) = I_4 \cos\left(\frac{\|\boldsymbol{\omega}\|\Delta t}{2}\right) + \frac{1}{\|\boldsymbol{\omega}\|}\sin\left(\frac{\|\boldsymbol{\omega}\|\Delta t}{2}\right)\Omega(\boldsymbol{\omega}) \tag{16}$$

where I_4 is a 4x4 identity matrix.

If the bias term is included in the formulation of the quaternion propagation, i.e., $\hat{\boldsymbol{\omega}} = \boldsymbol{\omega} - \boldsymbol{\varepsilon}$, where $\boldsymbol{\varepsilon}$ is a vector of gyro biases, then a system state composed by quaternions and gyro biases will have the following transition matrix [3]:

$$\Phi = \begin{bmatrix} \Phi_q & \Psi \\ 0_{3x4} & I_{3x3} \end{bmatrix} \tag{17}$$

where $\Psi = -\frac{1}{2}\int_{t_o}^{t} \Phi_q \Xi \, dt$ and the Ξ matrix is given by:

$$\Xi = \begin{bmatrix} q_4 & -q_3 & q_2 \\ q_3 & q_4 & -q_1 \\ -q_2 & q_1 & q_4 \\ -q_1 & -q_2 & -q_3 \end{bmatrix} \tag{18}$$

Note that the system is still linear with respect to system state composed by quaternions and biases. Therefore the transition matrix also assures the needed coupling between quaternions and biases to be taken into account in the covariance computations.

With such considerations, the quaternion approach makes the system dynamics to be fully linear. Thus in the prediction of state and covariance cycle, the conventional linear Kalman filter can be used so that it saves processing cost. Only the measurement equations are still non linear, and the Unscented transformation should be used, with the corresponding sigma-point measurement update cycle being implemented in the UKF. In this work, the state vector will be compose by four quaternions components and three gyro bias components,

$$\mathbf{x} = \left[\mathbf{q}\ \boldsymbol{\varepsilon}\right]^{T} \tag{19}$$

4. The Measurement System of the Satellite

In order to measure the satellite attitude accurately, several types of sensor, including gyros, earth sensors and solar sensors, are used in the measurement system. The mathematical models of these sensors are introduced here, and will compose the measurement vector of Eq. (6), given by

$$\mathbf{y} = \left[\phi_{H}\ \theta_{H}\ \alpha_{\psi}\ \alpha_{\theta}\right]^{T} \tag{20}$$

4.1. Mathematical Models of Gyros

The advantage of a gyro is that it can provide the angular displacement and/or angular velocity of the satellite directly. However, gyros have an error drifting problem, meaning that their measurement error increases with time. In this work, the RIGs (Rate-Integration Gyros) are used to measure the angular velocity of the roll, pitch and yaw of the satellite. Suppose the measurement error of a gyro consists of a constant drift ε and white noise η. The mathematical model of RIGs is [2]:

$$\Delta\boldsymbol{\Theta}_{i} = \int_{0}^{\Delta t} \left(\boldsymbol{\omega}_{i} + \boldsymbol{\varepsilon}_{i} \right) dt \qquad \left(i = x, y, z \right) \tag{21}$$

where $\Delta\boldsymbol{\Theta}$ are the angular displacement of the satellite in a time interval Δt. Thus, the estimated components of the angular velocity of the satellite are given by:

$$\hat{\boldsymbol{\omega}} = \mathbf{g} - \hat{\boldsymbol{\varepsilon}} - \hat{\eta} \tag{22}$$

where $\mathbf{g} = \left(\Delta\boldsymbol{\Theta} \big/ \Delta t \right)$ is the output vector of the gyroscope.

4.2. Mathematical Models of Infrared Earth Sensors (IRES)

One way to compensate for the drifting errors present in gyros is to use the earth sensors. These sensors are located on the satellite and aligned with their axes of *roll* and *pitch*. In the work, two

earth sensors are used, with one measuring the roll angle and the other measuring the pitch angle. In principle, an earth sensor cannot measure the *yaw* angle.

The measurement equations for the earth sensors are given as [2]

$$\begin{aligned} \phi_H &= \phi + b_\phi \\ \theta_H &= \theta + b_\theta \end{aligned} \tag{23}$$

where b_ϕ and b_θ are the *bias* representing the misalignment, installation and/or assembly.

4.3. Mathematical Models of Digital Solar Sensors (DSS)

The Solar Sensor is an optical mechanism that detects the Sun and sets the position of one of the main axes of symmetry of the spacecraft relative to the direction in which the Sun was detected. The Digital Solar Sensor of the CBERS-2 is not able to measure the *yaw* angle, this is, and these sensors do not provide direct measures. It measures the coupled *pitch* angle (α_θ) and *yaw* angle (α_ψ). The equations of measurements for DSS are obtained as follows [1,2].

$$\alpha_\psi = \tan^{-1}\left(\frac{-S_y}{S_x\cos(60^\circ)+S_z\cos(150^\circ)}\right)+\nu_{\alpha_\psi} \tag{24}$$

when $\left|S_x\cos(60^\circ)+S_z\cos(150^\circ)\right| \geq \cos(60^\circ)$, and

$$\alpha_\theta = 24^\circ - \tan^{-1}\left(\frac{S_x}{S_z}\right)+\nu_{\alpha_\theta} \tag{25}$$

when $\left|24^\circ - \tan^{-1}\left(\frac{S_x}{S_z}\right)\right| < 60^\circ$, where ν_{α_ψ} and ν_{α_θ} are the white noise representing the small remaining misalignment, installation and/or assembly errors. Just as the IRES, these errors are assumed Gaussian.

The conditions are such that the solar vector is in the field of view of the sensor, and S_x, S_y, S_z are the components of the unit vector associated to the sun vector in the satellite system and given by [1]:

$$\begin{aligned} S_x &= S_{0x} - \hat{\psi}S_{0y} - \hat{\theta}S_{0z} \\ S_y &= S_{0y} - \hat{\psi}S_{0x} - \hat{\phi}S_{0z} \\ S_z &= S_{0z} - \hat{\phi}S_{0y} - \hat{\theta}S_{0z} \end{aligned} \tag{26}$$

where S_{0x}, S_{0y}, S_{0z} are the components of the sun vector in the orbital coordinate system and $\hat{\phi}, \hat{\theta}, \hat{\psi}$ are the Euler angles estimated attitude.

5. Optimal Estimation of Satellite Attitude using a UKF and quaternion incremental

In this section the UKF algorithm is derived for attitude estimation. One approach for design of this filter involves using the quaternion kinematics in Eq. (15) directly. However, this approach has a clear deficiency. Mainly, referring to Eq. (4), since the predicted quaternion mean is derived using as averaged sum of quaternions, no guarantees can be made that the resulting quaternion will have unit norm. This makes the straightforward implementation of the UKF with quaternions undesirable. A solution for this problem is to use the quaternion incremental and the reduced representation of the covariance matrix.

The quaternion incremental is the quaternion which must be composed with the estimated quaternion in order to obtain the true quaternion. Since this quaternion incremental corresponds almost certainly to a small rotation, the fourth component will be close to unity and, hence, all the attitude information of interest is contained in the three vector components. Therefore, the state vector, $\delta\mathbf{x}$, related to quaternion incremental will be composed by the six components: three vector components of the incremental quaternion and three gyro bias components

5.1 Design of Unscented Attitude Filter

In order to make a better explication is shown the pseudocode of FKU with quaternion incremental.

- Parameters: **R** (considered known)
  Q (considered known)

- Initialization: $\hat{\mathbf{q}}_0$, $\hat{\boldsymbol{\varepsilon}}_0$

Covariance matrix related to Euler angles (φ) and gyro bias (ε): $\hat{\mathbf{P}}_0(\varphi,\boldsymbol{\varepsilon}) = \begin{bmatrix} \hat{\mathbf{P}}_0(\varphi) & \mathbf{0}_{3x3} \\ \mathbf{0}_{3x3} & \hat{\mathbf{P}}_0(\boldsymbol{\varepsilon}) \end{bmatrix}$

Covariance matrix related to quaternion (q): $\hat{\mathbf{P}}_0(q) = H\left(\partial q / \partial\varphi\right)\hat{\mathbf{P}}_0(\varphi)H^T\left(\partial q / \partial\varphi\right)$

Covariance matrix of state vector: $\hat{\mathbf{P}}_0(\mathbf{q},\boldsymbol{\varepsilon}) = \begin{bmatrix} \hat{\mathbf{P}}_0(\mathbf{q}) & \mathbf{0}_{4x3} \\ \mathbf{0}_{3x4} & \hat{\mathbf{P}}_0(\boldsymbol{\varepsilon}) \end{bmatrix}$

Reduced Covariance matrix of state vector: $\hat{\mathbf{P}}_0^r(\mathbf{q},\varepsilon) = S^T\hat{\mathbf{P}}_0(\mathbf{q},\varepsilon)S$, $S = \begin{bmatrix} \Xi(q) & \mathbf{0}_{4x3} \\ \mathbf{0}_{4x3} & I_3 \end{bmatrix}$

- Prediction Step:

State Vector Predicted: $\hat{\mathbf{q}}_{k+1}^{-} = \Phi_q(\Delta t, \boldsymbol{\omega})\ \hat{\mathbf{q}}_k$, $\hat{\boldsymbol{\varepsilon}}_{k+1}^{-} = \hat{\boldsymbol{\varepsilon}}_k$

$$\hat{\mathbf{x}}_{k+1}^{-} = \left[\hat{\mathbf{q}}_{k+1}^{-}\ \hat{\boldsymbol{\varepsilon}}_{k+1}^{-}\right]^T$$

Predicted Reduced Covariance matrix:

$$\hat{\mathbf{P}}_{k+1}^{r}(\mathbf{q},\varepsilon) = \tilde{\Phi}_{k+1,k}\,\hat{\mathbf{P}}_k^{r}(\mathbf{q},\varepsilon)\,\tilde{\Phi}_{k+1,k}^{T} + \int_{t_k}^{t_{k+1}} \tilde{\Phi}(t,t')\,\tilde{G}(t')Q(t')\tilde{G}^T(t')\,\tilde{\Phi}^T(t,t')dt'$$

with:

$$\tilde{\Phi}_{k+1,k} = \begin{bmatrix} \Lambda(t_{k+1},t_k) & K(t_{k+1},t_k) \\ \mathbf{0}_{3x3} & \mathbf{I}_3 \end{bmatrix}$$

$$\Lambda(t_{k+1},t_k) = \Xi^T(q(t))\,\Phi_q(t,t_0)\,\Xi(q(t_0)), \quad K(t,t_0) = -\frac{1}{2}\int_{t_k}^{t_{k+1}} \Lambda(t,t')\,dt'$$

$$\tilde{G}(t) \equiv S^T G(t) = \begin{bmatrix} -\frac{1}{2}\mathbf{I}_3 & \mathbf{0}_{3x3} \\ \mathbf{0}_{3x3} & \mathbf{I}_3 \end{bmatrix}$$

Reduced state vector: $\delta\hat{\mathbf{x}}_{k+1}^{-} \equiv \left[\delta\mathbf{q}\ \boldsymbol{\varepsilon}\right]^T = S^T\hat{\mathbf{x}}_{k+1}^{-}$, $\delta\mathbf{q} = \left[\delta\mathbf{q}\ 1\right]^T$

- Unscented Transformation: $\hat{\mathbf{q}}_{k+1}^{-}(i) = \delta\hat{\mathbf{q}}_{k+1}^{-}(i) \otimes \hat{\mathbf{q}}_{k+1}^{-}$

$$\Upsilon_{k+1}(i) = \left[\phi_H(i)\ \theta_H(i)\ \alpha_\psi(i)\ \alpha_\theta(i)\right],\ i=1,...,13$$

- Measurement Update: $\hat{\mathbf{y}}_{k+1} = \sum_{i=0}^{2n} W_i\left(\boldsymbol{\Upsilon}_{k+1}\right)_i$, i=1,…,13

$$\delta\hat{\boldsymbol{x}}_{k+1} = \delta\hat{\boldsymbol{x}}_{k+1}^{-} + K_{k+1}\left(\boldsymbol{y}_{k+1} - \hat{\boldsymbol{y}}_{k+1}^{-}\right)$$

with: $K_k = P_{xy}P_{yy}^{-1}$,

$$P_{xy} = \sum_{i=0}^{2n} W_i\left[(\boldsymbol{\chi}_k)_i - \hat{\boldsymbol{x}}_k^{-}\right]\left[(\boldsymbol{Y}_k)_i - \hat{\boldsymbol{y}}_k^{-}\right]^T, \quad P_{yy} = \sum_{i=0}^{2n} W_i\left[(\boldsymbol{Y}_k)_i - \hat{\boldsymbol{y}}_k^{-}\right]\left[(\boldsymbol{Y}_k)_i - \hat{\boldsymbol{y}}_k^{-}\right]^T + R$$

$$\mathrm{P_k} = \mathrm{P_k^-} - K_k\,\mathrm{P_{yy}}\,K_k^T$$

Quaternion updated: $\hat{\mathbf{q}}_{k+1}(i) = \delta\hat{\mathbf{q}}_{k+1}(i) \otimes \hat{\mathbf{q}}_{k+1}^{-}$

State Vector updated: $\hat{\mathbf{x}}_{k+1} = \left[\hat{\mathbf{q}}_{k+1}\ \hat{\boldsymbol{\varepsilon}}_{k+1}\right]^T$

6. Results

Here, the results and the analysis from the algorithms developed to estimate the attitude are presented. To validate and to analyze the performance of the estimators, real sensors data from the CBERS-2 satellite were used. The CBERS-2 satellite was launched on October 21st, 2003. The measurements are for April 21st, 2006, available to the ground system at a sampling rate of about 8.56 seconds for around 10 minutes of observation.

Indeed the on-board ACS (Attitude Control System) has full access to the sensor measurements sampled at the rate of 4Hz for the three gyros, to axes x, y, z of satellite; 1Hz for two Infrared Earth Sensors to the angle ϕ (*roll*) and θ (*pitch*); and 0.25Hz for two Digital Solar Sensors, related to the angles of pitch (α_θ) and yaw (α_ψ). However, owing to limited downlinked TM (telemetry), the ground system can recover telemetries for the sensors at around 9 seconds sampling and only during the satellite fly over the tracking station. This means that the ground system does not have the whole set of measurements available to the on-board ACS [6].

In total, it has been a set of 54 measurements from 13h 46min 25s until 13h 55min 27s, and measurements are spaced by 10s on average. For ease visualization measurements of the DSS and IRES sensors in Fig.1 and measurements the gyroscope in Fig.2 are graphically represented.

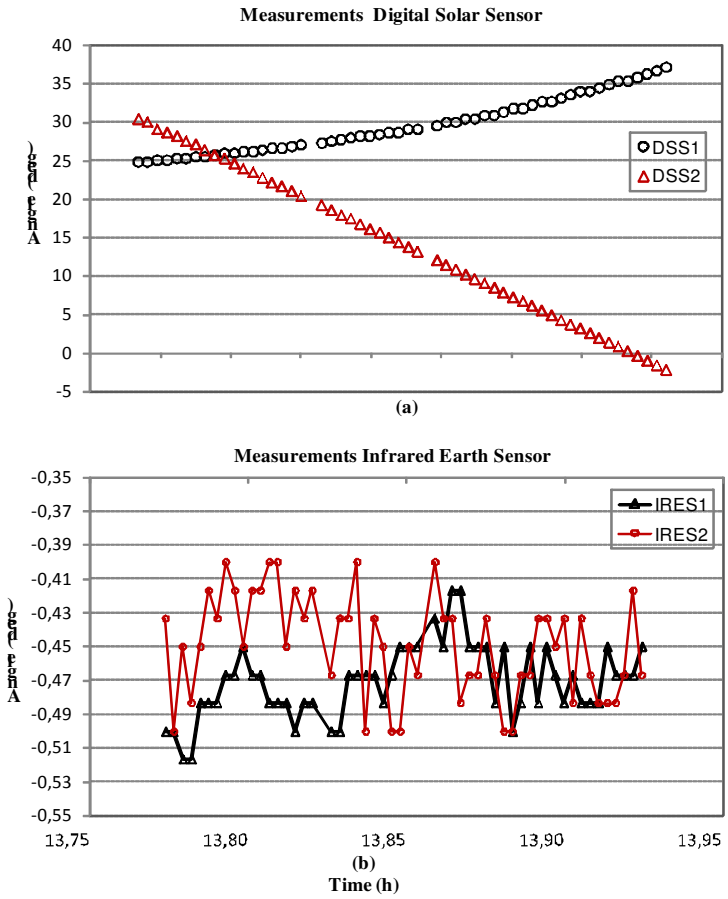

Figure 1. Representation of the real data from the sensors DSS and IRES from CBERS-2

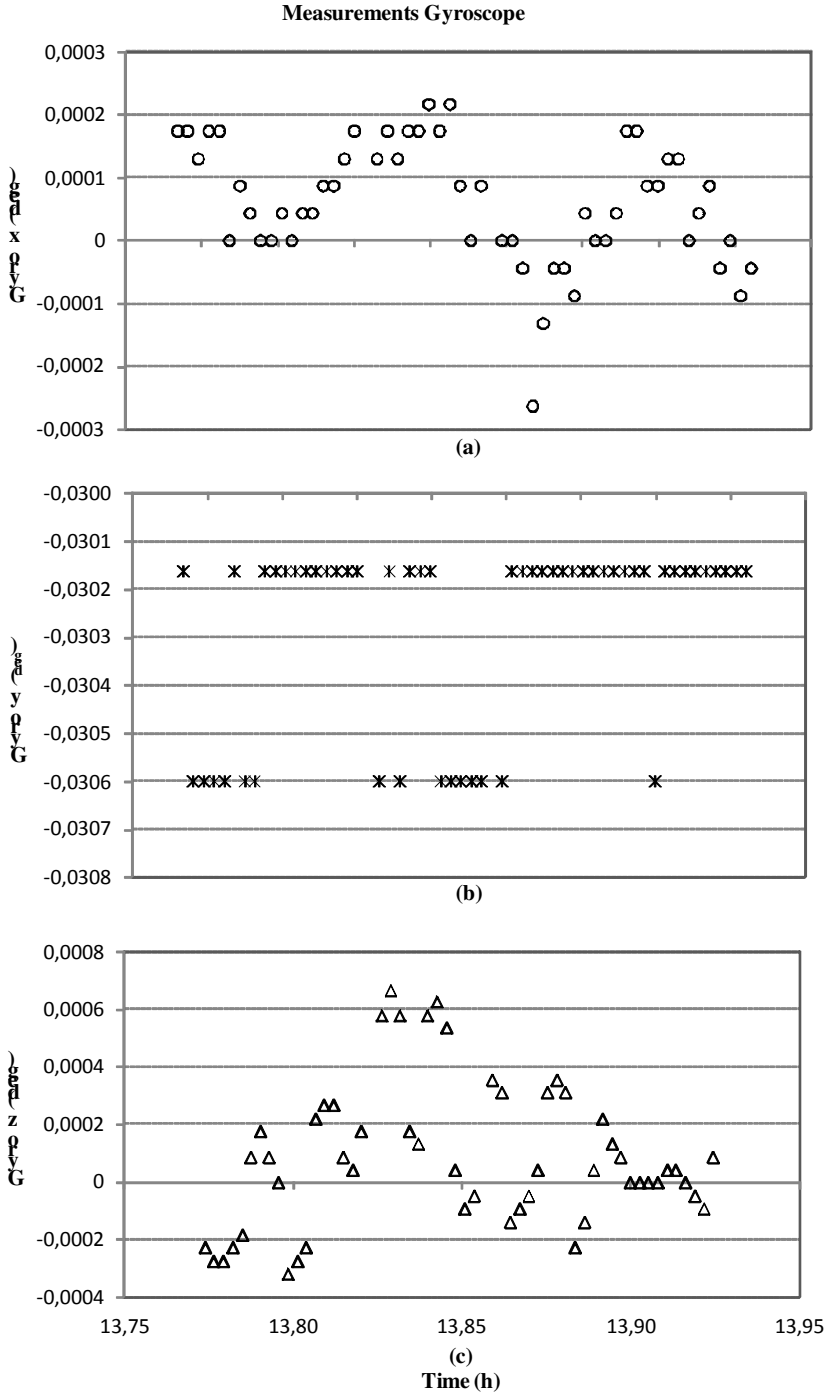

Figure 2. Representation of the real data of the gyroscope from CBERS-2

The algorithm implementation for the state estimation by the UKF using the quaternion incremental for the attitude representation was performed using MatLab® software. Due to fact that this study uses real data, and not simulated, it is necessary to validate the results with other

known. In this work the attitude estimation results obtained by the UKF are compared with the results obtained by LSM. According to the characteristics of the satellite and sensors, the parameters are listed as follows:

Table 1. Initial conditions of the state vector components

ϕ (deg)	θ (deg)	ψ (deg)	ε_x (deg/h)	ε_y (deg/h)	ε_z (deg/h)
0	0	0	5,76	4,64	2,68

Table 2. Values of the main diagonal of the initial covariance matrix (P)

σ_ϕ (deg)	σ_θ (deg)	σ_ψ (deg)	$\sigma_{\varepsilon x}$ (deg/h)	$\sigma_{\varepsilon y}$ (deg/h)	$\sigma_{\varepsilon z}$ (deg/h)
0,5	0,5	2,0	1,0	1,0	1,0

Table 3. Values of the main diagonal of the covariance matrix of the observation error (R)

σ_{DSS1} (deg)	σ_{DSS2} (deg)	σ_{IRES1} (deg)	σ_{IRES2} (deg)
0,6	0,6	0,06	0,06

Table 4. Values of the main diagonal of the covariance matrix of the dynamic noise (Q)

σ_x (deg)	σ_y (deg)	σ_z (deg)	σ_{Dgx} (deg/h)	σ_{Dgy} (deg/h)	σ_{Dgz} (deg/h)
0,1	0,1	0,1	0,01	0,01	0,005

In Fig. 3 and 4 it is observed the behavior of attitude and the *biases* of gyros during the period analyzed. The estimated attitude using increments of quaternions with UKF, Fig. 3, are close of the attitude reference values (LSM). The mean estimate to *roll* and *pitch* are in the order of -0.47 deg and -0.45 deg, respectively, for both estimators (UKF and LSQ). For *yaw* a random shape is not observed and its mean value is around -1.50 deg for UKF and -1.15 deg for LSM. In Fig. 4 it is observed the bias estimates behavior by the UKF. Due to shortage of measures, the analysis period was not sufficient for the convergence of the gyro bias.

The results of the residues DSS and IRES are shown in Fig.5 and Fig.6. The residuals are obtained by the difference between the calculated value and the measured value after the updating of the filter. It is considered that accuracy of DSS is smaller than IRES. It is observed that the behaviors of residues of DSS sensors are within the range of accuracy set by DSS (0.6 deg). However, on the case of IRES is observed that a more rapid convergence to zero exists.

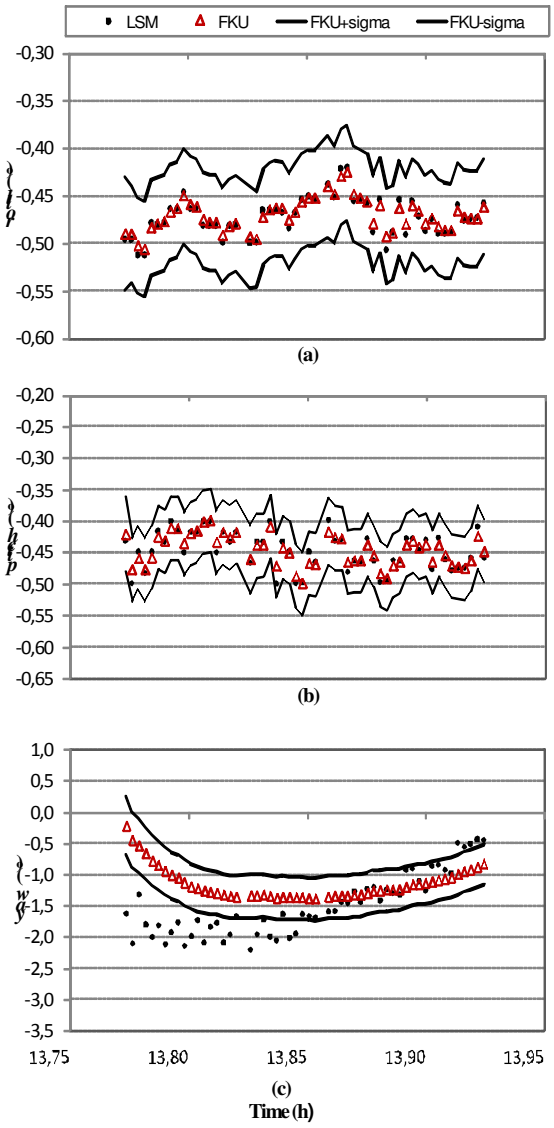

Figure 3. Estimated attitude

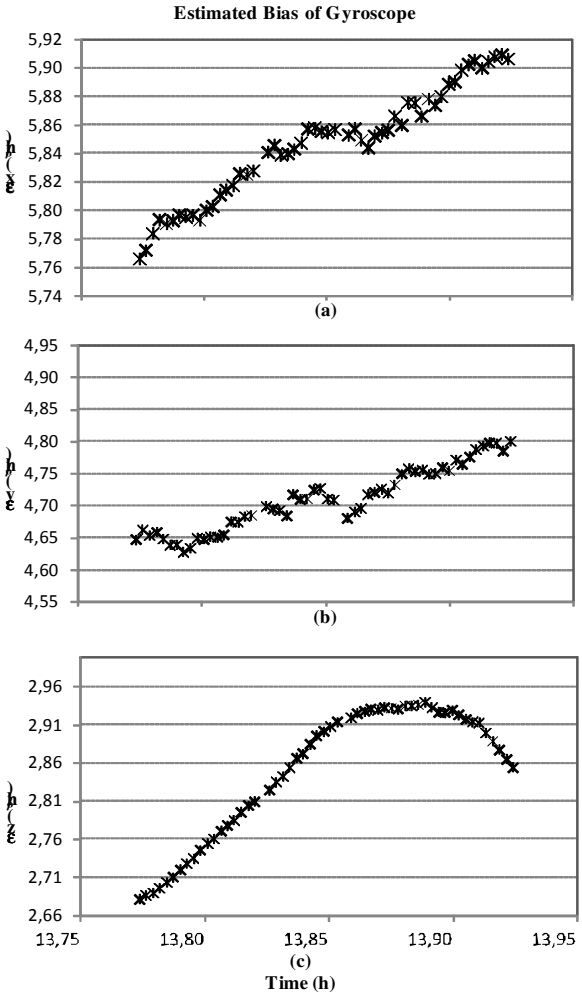

Figure 4. Estimated gyros bias

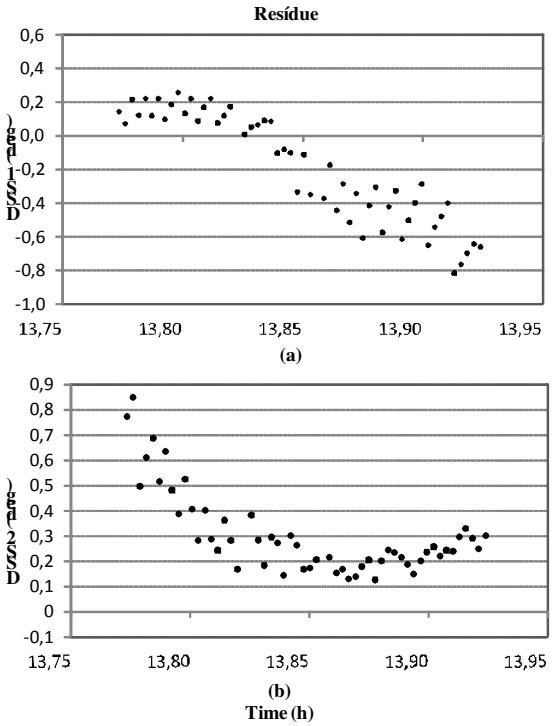

Figure 5. Residuals of Digital Sun Sensors

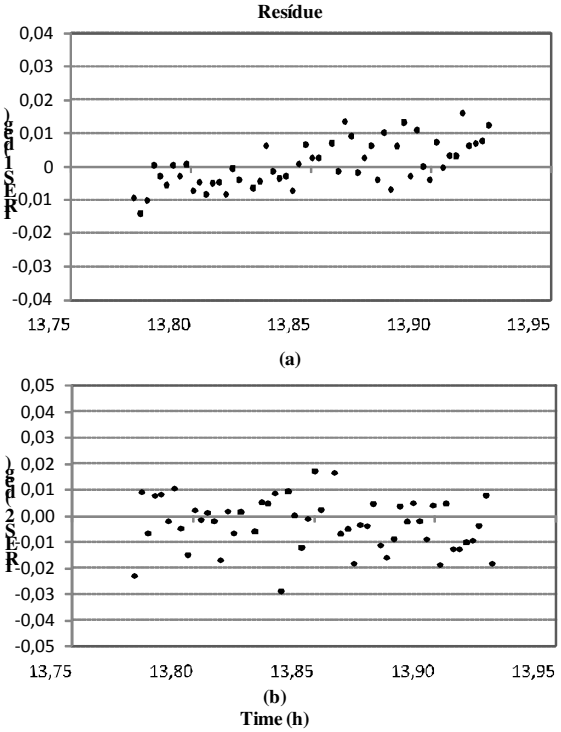

Figure 6. Residuals of Infrared Earth Sensors

7. Conclusions

The main objective of this study was to estimate the attitude of the satellite like CBERS-2, using real data, provided by sensors that are on board the satellite, the quaternion incremental and the Unscented Kalman Filter.

Although quaternions need 4 components with one redundancy when used in attitude estimation problems via UKF such parameterization makes the dynamical modeling linear. Therefore the overhead due to the unscented transformation to generate the sigma-points appears only in the measurement update cycle of the filter, where the measurement model is still nonlinear. This, in principle, translates to a computational saving because a numerical integration of $(2n+1)$ sets of differential equations for the dynamics are avoided (n being the number of filter states), which is mandatory when using Euler angles. On the other hand, not only the number of states to be estimated increases but also the covariancel. To solve this problem proposed by [5] a reduction in the order of the covariance matrix and state vector is made.

To verify the consistency of estimator, the attitude was compared with results obtained by a least square method (LSM). The usage of real data from on board attitude sensors, poses difficulties

like mismodelling, mismatch of sizes, misalignments, unforeseen systematic errors and post-launch calibration errors.
It is observed that the attitude estimated by the UKF is in close agreement with the results obtained by the LSM. It can be concluded that the algorithm of the UKF converges to the least squares solution, providing a kinematic attitude solution besides estimating biases.

8. Acknowledgments

The authors would like to thank the financial support received by FAPESP (2012/21023-6) and CAPES.

9. References

[1] Fuming, H.; Kuga, H. K., "CBERS Simulator Mathematical Models." CBTT Project, CBTT /2000 /MM /001. INPE, São José dos Campos, 1999.

[2]Garcia, R. V., "Filtro Não-Linear de Kalman Sigma-Ponto com Algoritmo Unscented Aplicado a Estimativa Dinâmica da Atitude de satélites Artificiais". Tese de doutorado, INPE, São José dos Campos, 2011.

[3] Garcia, R. V., Kuga, H. K., Zanardi, M. C., "Unscented Kalman Filter for Spacecraft Attitude Estimation Using Quaternions and Euler Angles". 22nd International Symposium on Space Flight Dynamics, São José dos Campos, 2011.

[4] Julier, S. J.; Uhlman, J. K., "A new extension of the Kalman filter to non linear systems." Proceedings of the International symposium on aerospace/defense sensing, simulation and controls, Orlando, FL, 1997.

[5] Lefferts, E. J.; Markey, F. L.; Shuster, M. D., "Kalman Filtering for Spacecraft Attitude Estimation." Journal of Guidance, Control and Dynamics, Vol. 5, No. 5, pp. 417-429, 1982.

[6] Lopes, R.V.F.; Kuga, H. K., "CBERS-2: On Ground Attitude Determination from Telemetry Data." São José dos Campos, INPE, Internal Report C-ITRP, 2005.

[7] Pisacane, V. L.; Moore, R. C., "Fundamentals of Space Systems." Oxford University Press, NY, 1994.

[8] Wertz, J. R., "Spacecraft Attitude Determination and Control," D. Reidel, Dordrecht, Holland, 1978.